Astronomy & Astrophysics manuscript no. hd102077˙arxiv
March 26, 2014
© ESO 2014

The young binary HD 102077: Orbit, spectral type, kinematics, and moving group membership⋆

Maria Wöllert[1], Wolfgang Brandner[1], Sabine Reffert[2], Joshua E. Schlieder[1], Maren Mohler-Fischer[1], Rainer Köhler[1], and Thomas Henning[1]

[1] Max-Planck-Institut für Astronomie, Königstuhl 17, 69117 Heidelberg, Germany
e-mail: woellert@mpia.de
[2] Landessternwarte, Königstuhl 12, 69117 Heidelberg, Germany

Received —; accepted —

ABSTRACT

The K-type binary star HD 102077 was proposed as a candidate member of the TW Hydrae Association (TWA) which is a young (5 − 15 Myr) moving group in close proximity (∼ 50 pc) to the solar system. The aim of this work is to verify this hypothesis by different means. We first combine diffraction-limited observations from the ESO NTT 3.5 m telescope in SDSS-i' and SDSS-z' passbands (three epochs) and ESO 3.6 m telescope in H-band (one epoch) with literature data to obtain a new, amended orbit fit of the visual binary. We then estimate the spectral types of both components from the i'-z' colours and reanalyse the Hipparcos parallax and proper motion taking the orbital motion into account. Moreover, we use two high-resolution spectra of HD 102077 obtained with the fibre-fed optical echelle spectrograph FEROS at the MPG/ESO 2.2 m telescope to determine the radial velocity and the lithium equivalent width of the system. Finally, we use all the information to discuss the kinematic properties of HD 102077 and to estimate the age of the system.

The orbital elements of the HD 102077 trajectory are well constrained and we derive a total system mass of $2.6 \pm 0.8\,M_\odot$ and a semi-major axis of 14.9 ± 1.6 AU. From the i'-z' colours we infer an integrated spectral type of K2V, and individual spectral types of $K0 \pm 1$ and $K5 \pm 1$ for primary and secondary, respectively. The radial velocity corrected for the orbital motion of the system is 17.6 ± 2 km/s. Even though the parallax determination from the Hipparcos data is not influenced by the orbital motion, the proper motion changes to $\mu_\alpha * \cos\delta = -137.84 \pm 1.26$ mas yr^{-1} and $\mu_\delta = -33.53 \pm 1.45$ mas yr^{-1}. With the resultant space motion, the probability of HD 102077 being a member of TWA is less than 1%. Furthermore, the lithium equivalent width of 200 ± 4 mÅ is consistent with an age between 30 Myr and 120 Myr and thus older than the predicted age of TWA. The comparison of HD 102077's temperature and luminosity to isochrones supports this result. In conclusion, HD 102077's age, galactic space motion, and position do not fit TWA or any other young moving group.

Key words. Instrumentation: high angular resolution – Astrometry – binaries: general – Stars: fundamental parameters – Stars: late-type – Stars: individual: HD 102077

arXiv:1403.6280v1 [astro-ph.SR] 25 Mar 2014

1. Introduction

The TW Hya association (TWA) is a loose group of stars (Gregorio-Hetem et al., 1992) that have common galactic kinematics, age, and origin (Kastner et al., 1997; Weinberger et al., 2013). The association has 22 high probability members with individual distances between 28 pc and 70 pc (Torres et al., 2008). The age of its members has been estimated using different indicators of youth such as activity and lithium abundance as well as their position in the Hertzsprung-Russell diagram and is about 10 ± 5 Myr (Weinberger et al., 2013). Young, nearby associations like TWA are of great importance to understanding the local star forming history, and provide a sample of young stars, brown dwarfs, and planets for high-resolution studies. Therefore, several groups have been looking for additional members (Schlieder et al., 2010, 2012; Zuckerman et al., 2011; Shkolnik et al., 2012; Rodriguez et al., 2013; Malo et al., 2013; Moór et al., 2013).

The binary HD 102077 (also called HIP 57269, V 838 Cen, and RST 3558AB) was proposed as a candidate member of TWA based on its kinematics by Makarov & Fabricius (2001). Kinematic candidate members, however, need to be verified by spectroscopic measurements. The first spectroscopic follow up was done by Song et al. (2002), who measured the Li 6708 Å strength of HD 102077. They find a fairly large equivalent width of 196 mÅ, which is a strong indication of a young system. The authors argue, however, that an age of more than 30 Myr is more likely and thus do not consider HD 102077 as a new member of TWA. Apart from the lithium absorption line, HD 102077 shows strong X-ray emission which also hints at a young age (Makarov, 2003). The WISE data (Cutri & et al., 2012) shows, however, no infrared excess and thus no sign of a disk. Even though HD 102077 is a young star, several research groups have assigned it low metallicity values. Holmberg et al. (2007) used the Stroemgren UVBY photometry by Olsen (1994) to derive a [Fe/H] of −0.9. Casagrande et al. (2011) redid their analysis and find [Fe/H]= −0.76. An independent metallicity measurement was done by Randich et al. (1993). They fitted spectral templates to high-resolution spectra with $R = 50000$ over the region of $\approx 6680 - 6730$ Å and obtained [Fe/H]= −0.4. The photometric determination of the metallicity content is not very accurate because of HD102077s binarity and variability and this may be the cause of the discrepancy. For instance, Cutispoto (1990) mea-

⋆ Based on observations made with ESO Telescopes at the La Silla Paranal Observatory under programme IDs 084.D-0669(A), 088.C-0753(A), 091.D-0494(A), 53.7-0107, 091.A-9013(A).

sured the $UBVRI$ colours over several photometric phases and observed that $U - B$ varies by 0.04 mag and that the star gets bluer at light maximum. Even stronger variations have been observed by Udalski & Geyer (1985). They find brightness changes of 0.08 mag with a probable period of 1.84 or 2.2 days. Since the V-band lightcurves at different epochs differ greatly in shape and mean magnitude (Cutispoto, 1990, 1993, 1998) the starspot size and distribution seem to vary considerably. Duplicity of one of the two components could also add to the observed variations.

König et al. (2003) measured the radial velocity of the system and find that the space motion is quite different from the average space velocity of TWA. Nevertheless, they point out that the distance of HD 102077, its location in the sky, its spectral type, its position in the H-R diagram, its $v \sin i$, and X-ray emission are very similar to other confirmed TWA members. This group also presents evidence of a third component in the system. The proposed star is at a distance of 8.46″ from the primary and it shows calcium and lithium absorption. The lithium EW of 0.18 ± 0.2 Å and a spectral type of $K5 \pm 1$ point to a similar age to the A component. We checked the imaging archives to see whether there is an indication of common proper motion. The stars do seem to move together with respect to the background stars in the field when comparing an R-band image from 1983 to an R-band image from 1992 and the 2MASS K-band image from 1999. The psfs are, however, blended in all these images and thus no quantitative proper motion measurement is possible. Nevertheless, the calcium and lithium absorption features as well as the likely common proper motion is strong evidences of a bound system.

The integrated spectral type of HD 102077 of $K0/1Vp$ was first determined by Anders et al. (1991) by high-dispersion observations of the Li 6707 Å doublet and König et al. (2003) find $K1/2$ using DFOSC at the 1.54 m Danish telescope. The spectral type of the primary components is, however, less clear. Fabricius & Makarov (2000) analysed the Hipparcos Tycho data and find that the brighter component has a redder B-V colour, corresponding to spectral types K4 and K2, but they do not give an explanation for this unexpected result. Cutispoto (1998) uses the UBVRI colours of the integrated system and ΔH_p from the Hipparcos satellite catalog to classify HD 102077 as consisting of a $K0/1V$ and a $K5V$.

The source HD 102077 is a visual binary star and thus allows the determination of the total system mass. The first orbital parameters were derived by Heintz (1986). His best fit to data from seven epochs is a low eccentricity orbit with a period of 32.35 years and a semi-major axis of 0.28″. At that time, the parallax of HD 102077 was not known. Therefore, Heintz used Kepler's Third Law and the mass-luminosity relation to estimate the dynamical parallax. He obtained 42.3 pc and deduced a total system mass of 1.6 $M_{\odot}$.

In this paper, we present the results of our astrometric, photometric, and spectroscopic study of HD 102077. We derive a new orbit fit of the binary system, and we determine the i'-z' colours and from these the spectral types of the individual components. We measure the radial velocity and the lithium equivalent width of the system. Finally, we use these results to discuss a possible TWA membership of HD 102077.

2. Observations and data reduction

2.1. Literature data

The source HD 102077 has been observed in the optical with various telescopes and instruments since 1929 (see Table 1).

Table 1. Astrometric measurements of HD 102077

Date	PA [°]	ρ ["]	Ref
1929.065	348.9 ± 5.0	0.24 ± 0.1	Ro
1949.529	270.0 ± 5.0	0.17 ± 0.1	Ro
1964.32	60.5 ± 5.0	0.19 ± 0.1	Ho
1976.125	164.4 ± 5.0	0.14 ± 0.1	Wo
1980.231	243.5 ± 5.0	0.14 ± 0.1	Wo
1983.168	264.6 ± 5.0	0.19 ± 0.1	Wo
1985.34	278.5 ± 5.0	0.33 ± 0.1	He
1989.3059	298.7 ± 0.2	0.416 ± 0.003	Mc
1990.3462	302.9 ± 0.2	0.42 ± 0.003	Ha
1991.25	306 ± 1.0	0.43 ± 0.006	Hi
1994.504	320.2 ± 0.7	0.418 ± 0.004	*
2001.0825	352.9[a] ± 0.7	0.335 ± 0.004	Ma
2009.2598	115.5 ± 0.3	0.1795 ± 0.001	To
2010.08	135.9 ± 0.5	0.183 ± 0.003	*
2011.0373	157.3[a]±0.2	0.1874±0.002	Hk
2012.011	177.3 ± 0.5	0.196 ± 0.003	*
2013.3042	202.9 ± 0.7	0.21 ± 0.003	*

Ro: Rossiter (1955), Ho: Holden (1965), Wo: Worley (1978), He: Heintz (1986), Mc: McAlister et al. (1990), Ha: Hartkopf et al. (1993), Hi: ESA (1997), Ma: Mason et al. (2011), To: Tokovinin et al. (2010), Hk: Hartkopf et al. (2012), *: This work, a: position angle corrected by 180°

All measurements until 1985 were done with a filar micrometer. Because of the small separation of the two components close to the resolution limit of the telescopes used, we adopt a high uncertainty in the separation of 0.1″ and 5° in the position angle for all micrometer measurements. The uncertainties of the later measurements are the values reported by the authors in the papers or in follow-up studies. We note that the binary was not resolved by Worley in 1972 nor by Heintz in 1984 (Heintz, 1986).

2.2. AO observation with COME-on+/SHARPII

The observations of HD 102077 in the H-band were obtained on July 2, 1994, with the adaptive optics (AO) system ComeOn+ (Rousset et al., 1994) and the near-infrared camera Sharp2 (Hofmann et al., 1992) at the ESO 3.6 m telescope in La Silla, Chile. For sky subtraction, HD 102077 was observed in two different quadrants of the detector with 30 individual frames each. Exposure times of the single frames were 1 s. The star positions for both configurations were measured with IRAF imexamine assuming a two-pixel object radius. Their values were averaged, and the standard deviation was used to estimate measurement uncertainties.

Astrometric calibrations were achieved through observations of the astrometric binary IDS 17430S6022 (van Dessel & Sinachopoulos, 1993). These observations yield an image scale of 50.20 ± 0.12 mas/pixel and show that the y-axis of the detector was aligned with the north direction to within ±0.20 deg.

2.3. Lucky Imaging with AstraLux

Three additional epochs were obtained using the Lucky Imaging camera AstraLux Sur at the ESO 3.5 m New Technology Telescope at La Silla (see Hormuth et al., 2008; Hippler et al., 2009, for more information on AstraLux). Lucky Imaging is a passive technique which enables nearly diffraction-limited observations on 2- to 4-meter telescopes. The seeing is reduced by

taking a series of many short exposures of the target and combining only the least distorted frames to the final image.

We observed HD 102077 on February 7, 2010; on January 2, 4, and 5, 2012; and on April 21, 2013. At each time we imaged HD 102077 in i'- and z'-passband except on January 4, 2012, when we only took a z'-band image, and January 2, 2012 when we observed HD 102077 in z'-band twice. The z'-band image from January 5, 2012, is shown in Fig. 1 as an example. The exposure time of individual frames was 30 ms in 2010 and 15 ms on the other dates. In order to match a total integration time of 300 s, the number of integrations was set to 10000 and 20000, respectively.

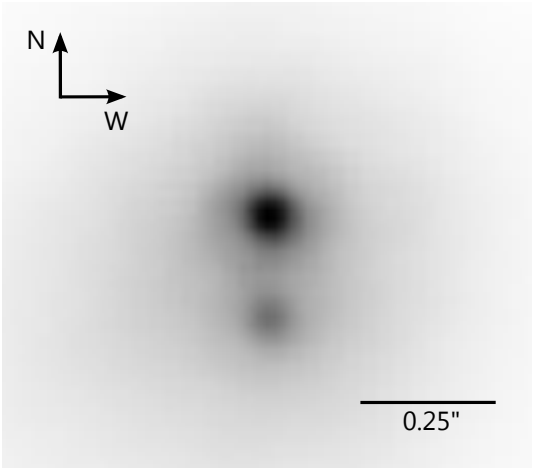

Fig. 1. z' filter image of HD 102077 with AstraLux at La Silla observatory from January 5, 2012. The image scale is linear.

The single frames were corrected for electronic offset and differences in pixel sensitivity using a masterflat and -bias, respectively. After noise filtering and resampling the pixel scale from 30.5 mas/pixel to 15.25 mas/pixel, the Strehl ratio of the point spread function was measured. Only 1% of the images with the highest Strehl ratio were then combined to the final image. The assembling is based on the Drizzle algorithm (Fruchter & Hook, 2002). It shifts the selected images such that the brightest pixel of the reference star is always positioned at the same pixel coordinates.

Astrometric reference stars in the open cluster NGC 3603 were observed each night to calibrate the detector rotation and pixel scale. We measured the detector position for five stars of NGC 3603 with IRAF imexamine, calculated the separation and rotation angle pairwise, and compared these values to data from high-quality astrometric HST/WFP2 observations (Rochau et al., 2010). This analysis yielded a plate scale of 15.25 ± 0.03 mas/px, 15.25 ± 0.01 mas/px, and 15.24 ± 0.02 mas/px and a detector rotation of 1.8° ± 0.2°, 2.1° ± 0.2°, and 3.8° ± 0.2° west of north in 2010, 2012, and 2013 respectively. Additionally, twilight sky-flats and bias were measured in both filters at the beginning of each observing night.

The positions of the binary components as well as their magnitude differences in the i' and z' filters were obtained by fitting a model psf to the data. The co-adding of images of short exposures with random atmospheric distortions is described by (Hormuth et al., 2008):

$$\mathrm{PSF}_{\mathrm{obs}}(r) = W\left(\frac{1}{r^2/\sigma_m^2+1}\right)^{\beta} + (1-W)\left(\mathrm{PSF}_{\mathrm{th}}(r) * \frac{1}{\sqrt{2\pi\sigma_g^2}}\exp\left(-\frac{r^2}{2\sigma_g^2}\right)\right). \quad (1)$$

On the right-hand side $\mathrm{PSF}_{\mathrm{th}}$ is the ideal point spread function without atmospheric turbulences and telescope aberrations, which is then convolved with a Gaussian blurring function of parameter σ_g. To obtain the observed PSF, a Moffat profile with parameters β and σ_m is added to the blurred theoretical profile; W weights the two PSF components. Our code determines all parameters simultaneously by a Levenberg-Marquardt least-squares fit to both binary components.

In order to unveil systematic errors of the code we constructed binaries from seven single stars that we imaged on the same night. The synthetic binaries had similar separation and brightness ratios to HD 102077, and were introduced at position angles of 0°, 45°, 90°, 135°, 180°, and 270°. We compared the fit results with the set system properties and found no systematic offset in separation, position angle, and flux ratio.

In addition to the flux ratio of the binary component aperture photometry with IRAF apphot was used for our observations from 2010 to determine the i' and z' magnitudes of the integrated system. We chose an aperture radius of 21 px centred on the primary star to ensure that most of the flux of both components is covered. The sky background was measured in an annulus from 25 px to 35 px. The corresponding photon flux is then calculated taking into account the system gain, the exposure time, the mirror area, and the quantum efficiency of our CCD in i' and z' passband which is 0.8 and 0.4, respectively. For an absolute calibration of the instrument we observed two astrometric standard stars at a comparable airmass during the same night and analysed them in the same way. To calibrate our instrument we only considered offsets between our instrumental magnitude and the standard value given in literature and no colour terms.

2.4. High-resolution spectroscopy with FEROS

Two high-resolution spectra of HD 102077 were obtained on July 26 and July 27, 2013, with the fibre-fed optical echelle spectrograph FEROS (Kaufer & Pasquini, 1998) at the MPG/ESO 2.2 m telescope at La Silla Observatory in Chile. FEROS covers the whole optical spectral range from 3600 Å to 9200 Å and provides a spectral resolution of ≈ 48000. The fibre aperture of FEROS is 2 arcsec and thus contains the light of both components. The exposure time of each spectrum was 1500 s and resulted in a signal-to-noise ratio of 223 and 192 at 5450 Å, respectively. The spectra were taken in the object-cal mode and were reduced with the online Data Reduction System (DRS) at the telescope. The reduction includes detection of spectral orders, wavelength calibration and background subtraction, flatfield correction and order extraction, as well as merging the individual orders after rebinning the reduced spectra to constant wavelength steps. Since the FEROS pipeline applies the barycentric correction inaccurately (Müller et al., 2013), we recalculated the barycentric correction with the IDL routine baryvel.pro including the rotation of Earth at the observatory.

The stellar parameters of HD 102077 are determined by fitting synthetic spectra to the stellar spectrum using the spectral synthesis code Spectrocopy Made Easy, *SME* (Valenti &

Piskunov, 1996). We use these stellar parameters to compute a template spectrum which we then cross-correlate with the measured spectrum to determine the radial velocity of the system. Furthermore, we measure the Li 6708 Å equivalent width.

3. Physical properties of the HD 102077 binary

3.1. Orbit determination

The orbit of a binary system can be characterized by the relative motion of the secondary around the primary. Even though we only see a projection of the movement on the celestial sky, a sequence of observations at many different epochs, preferably covering more than one complete orbit, makes it possible to determine all orbital elements. The astrometric data of HD 102077 covers more than two full orbits (see Table 1).

To find the best fit to that data we employ a grid-search in eccentricity e, period P, and time of periastron T_0. For every set of these values we solve the Kepler equation and we get the eccentric anomaly E for every point in time t that has been measured:

$$E - e \sin E = \frac{2\pi}{P}(t - T_0).$$

Then the elliptical rectangular coordinates of the real orbit X and Y are calculated at every epoch,

$$X = \cos E - e$$
$$Y = \sqrt{1 - e^2} \cdot \sin E,$$

and X and Y are connected with the measured projected points x, y via the four Thiele-Innes coefficients A, B, F, G:

$$x = A \cdot X + F \cdot Y$$
$$y = B \cdot X + G \cdot Y.$$

The Thiele-Innes coefficients in turn depend on the orbital elements, the semi-major axis a, the angle between node and periastron ω, the position angle of the line of nodes Ω, and the inclination i:

$$A = a(\cos\omega\cos\Omega - \sin\omega\sin\Omega\cos i)$$
$$B = a(\cos\omega\sin\Omega + \sin\omega\cos\Omega\cos i)$$
$$F = a(-\sin\omega\cos\Omega - \cos\omega\sin\Omega\cos i)$$
$$G = a(-\sin\omega\sin\Omega + \cos\omega\cos\Omega\cos i).$$

Using all epochs A, B, F, and G are calculated using singular value decomposition. Finally, the orbital elements can be computed. The goodness of every fit is measured with the χ^2 test. The minimal χ^2 corresponds to the best fit. The best orbital solution for HD 102077 has a reduced χ^2 of 2.6 and can be seen in Fig. 2; the corresponding orbital elements can be found in Table 2. Uncertainties were estimated by analyzing the χ^2 function around its minimum. The errors given in Table 2 represent the 68% confidence interval (see Köhler et al. (2008) for more details).

The semi-major axis of 14.9 ± 1.6 AU and the system mass of $2.6 \pm 0.8\,M_\odot$ were calculated using the revised Hipparcos parallax of 20.6 ± 2.1 mas. The uncertainties of these values are clearly dominated by the distance uncertainty. We note that we excluded the data point from 1964 for our orbital fit. It shows a significant and unexplainable offset compared to all other data points and we have no means to recheck its derivation. We also added 180° to the position angle measurements from 2001 and 2011 in order to match the other observations.

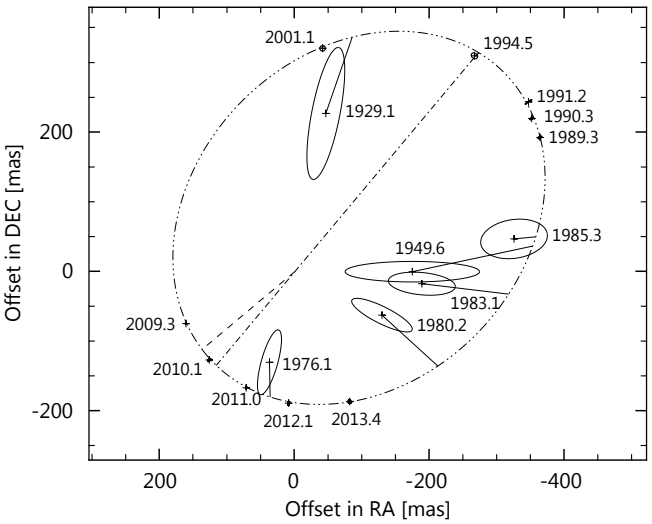

Fig. 2. Best fitting orbit of HD 102077 in the rest frame of the primary. The observed positions are marked by their error ellipses and lines connecting the observed and calculated positions at the time of the observation. The dash-dotted line indicates the line of nodes, the dashed line the periastron. We note that the micrometer measurements all tend to estimate a smaller projected separation.

Table 2. Parameters of the best orbital solution.

Orbital Element	Value
Date of periastron T_0 (JD)	2455142^{+4}_{-6}
Period P (years)	$35.5^{+0.3}_{-0.3}$
Semi-major axis a (mas)	$306.2^{+1.1}_{-1.4}$
Inclination i (°)	$28.5^{+0.4}_{-1.3}$
Eccentricity e	$0.409^{+0.004}_{-0.002}$
Argument of periastron ω (°)	$348.60^{+0.09}_{-0.91}$
P.A. of ascending node Ω (°)	$140.0^{+0.1}_{-1.3}$
System mass M_S ($M_\odot$/kpc^3)	22834^{+265}_{-359}
Semi-major axis a (AU)	$14.9^{+1.6}_{-1.6}$
System mass M_S ($M_\odot$)	$2.6^{+0.8}_{-0.8}$

3.2. Stellar parameters

3.2.1. i'-z' colours

The spectral type of the integrated system as well as the spectral types of the individual components are determined from i'-z' colours which we compare to the spectral type models for main-sequence stars by Kraus & Hillenbrand (2007). Even though HD 102077 may still be in its pre-main-sequence phase, it is reasonably close to the zero-age main sequence to justify the adoption of main-sequence colours and magnitudes. We derive an integrated spectral type of K2V. To determine the i'-z' colours of the individual components we need to disentangle their signal. This is achieved by fitting a theoretical PSF to both stars simultaneously. Averaging the results of all five z'-band images and three i'-band images we get a flux ratio of 0.377 ± 0.02 and 0.325 ± 0.01, respectively. Together with the apparent integrated

i'- and z'-magnitudes, this yields a spectral type of $K0 \pm 1$ for the primary and $K5 \pm 1$ for the secondary.

3.2.2. Spectra

In fitting model spectra to our binary system we find $T_{\rm eff} \approx 5265$ K, $\log g \approx 4$, Fe/H ≈ -0.37, and $v \sin i \approx 8.3$ km/s. However, these results should be taken with care since we only fit one component to the unresolved binary system. The lines are expected to be broadened from the relative motion of the two components which can be calculated from our orbit fit to be 5 ± 0.5 km/s in July 2013 when the spectra were taken. We find a radial velocity of 19.8 km/s with a small uncertainty of 0.1 km/s introduced by the measurement and larger uncertainty introduced by the orbital motion. The measured velocity lies between the radial velocity of the primary and the secondary and it depends on the mass ratio and on the flux ratio of the two components. Since the exact values are not known we adopt an uncertainty of 2.5 km/s, half of the relative speed, corresponding to the highest possible uncertainty.

We also calculated the radial velocity of the individual components with an IDL analysis package that is based on the 2D cross correlation technique described in Mazeh et al. (2002) (C. Bender, private communication). The cross correlation of the two spectra of HD 102077 with one K0 template gives 19.8 ± 0.4 km/s and confirms the above mentioned value. The simultaneous cross correlation with an K0 and an K5 template increases the correlation coefficient significantly and gives an individual radial velocity of 26.5 ± 0.9 km/s for the primary and 12.7 ± 0.7 km/s for the secondary in four different wavelength ranges and in both spectra. The radial velocity difference of about 14 km/s of the two components does not agree with the predicted value of 5 km/s from our orbit fit. This could be explained either by a third component in the system or by a parallax measurement that is too large by about a factor of 2.8. The second would, however, lead to an unreasonably high system mass of about 57 $M_\odot$. In addition, our reanalysis of the Hipparcos parallax does not suggest an incorrect parallax determination (see section 4.3).

3.3. V-band variability

We analysed the variability of HD 102077 by studying the Hipparcos V-band data. During the mission lifetime the satellite scanned 166 times over HD 102077. The observations span more than three years and thus have a much longer baseline than all previous measurements. To find repeating signals we calculated the generalized Lomb-Scargle periodogram (Zechmeister & Kürster, 2009) shown in Fig. 3. The highest power is obtained by a period of 4.04 days followed by a period of 1.8 days. These powers are, however, small and are most likely not associated with a real signal. To test whether the maximum peaks arose just by chance we deleted 20% of the data randomly and recalculated the periodogram; this procedure was repeated several times. Most often we find different prominent peaks. In addition, we analysed the light curve with two algorithms which do not assume a sinusoidal signal: a) box-fitting least squares (Kovács et al., 2002) which is optimized to find periodic transits, and b) Plavchan (Plavchan et al., 2008) which makes no assumption about the underlying periodic signal. Neither of these algorithms shows a solution with a high power and the most likely periods differ when deleting 20% of data randomly. This suggests that apart from the brightness variation of HD 102077 due to stellar activity as has also been seen in the shorter period observations (Cutispoto, 1990, 1993, 1998) no other signal can be detected in the Hipparcos data.

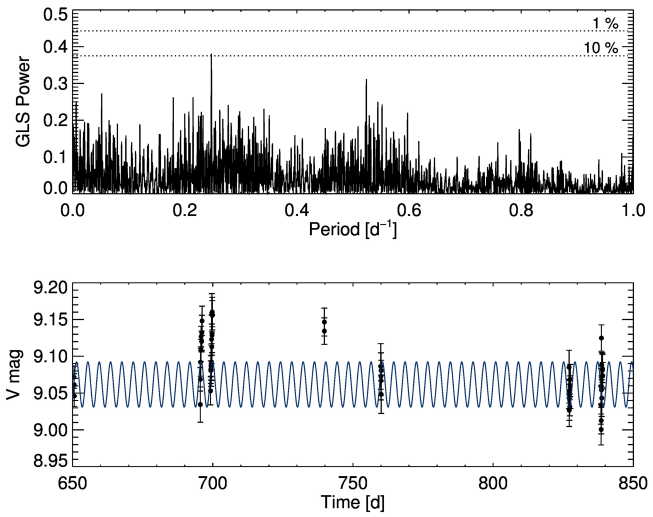

Fig. 3. Top: Generalized Lomb-Scargle periodogram for Hipparcos V-band data. Hte highest power is reached for a period of 4.04 days. The false alarm probability of 1 % and 10 % are indicated by the dotted lines. Bottom: A part of the Hipparcos light curve is overplotted with the most significant periodic signal.

3.4. Age estimate

3.4.1. Using isochrones

We use Pisa (FRANEC) pre-main-sequence isochrones (Tognelli et al., 2011) to estimate the age of HD 102077. The isochrones are computed for a fine grid of mass, age, metallicity, and helium abundance and give the bolometric luminosity as a function of the effective temperature of stars at a certain age. We deduce the effective temperature of HD 102077's two components from our spectral type estimates using the stellar SEDs of Kraus & Hillenbrand (2007). We find $\log T_{\rm eff} = 3.73^{+0.025}_{-0.015}$ for the primary and $\log T_{\rm eff} = 3.63^{+0.030}_{-0.022}$ for the secondary. We calculate the bolometric luminosity from the Tycho V_T and B_T colours of 9.44 mag and 10.50 mag for the primary and 10.56 mag and 11.47 mag for the secondary. We assume that the uncertainty of the Tycho-magnitudes is dominated by the stellar variability whose 1σvalue is 0.04 mag. Using the theoretical calibration from Tycho to Johnson magnitudes (Bessell, 2000) and the bolometric correction from Voigt (1988) we find a bolometric magnitude of $5.60^{+0.21}_{-0.23}$ mag for the primary and $6.33^{+0.21}_{-0.23}$ mag for the secondary. We now place both components in a H-R diagram (see Fig. 4) together with Pisa pre-main-sequence isochrones. As input parameters we use a metallicity value of -0.4 dex as was determined by Randich et al. (1993) and our own FEROS measurement and we assume solar helium mass fraction and mixing length. We overlayed stellar tracks for comparison. Both components lie above the main sequence, with an age between 25 Myr and 100 Myr for the primary, and 15 Myr and 50 Myr for the secondary.

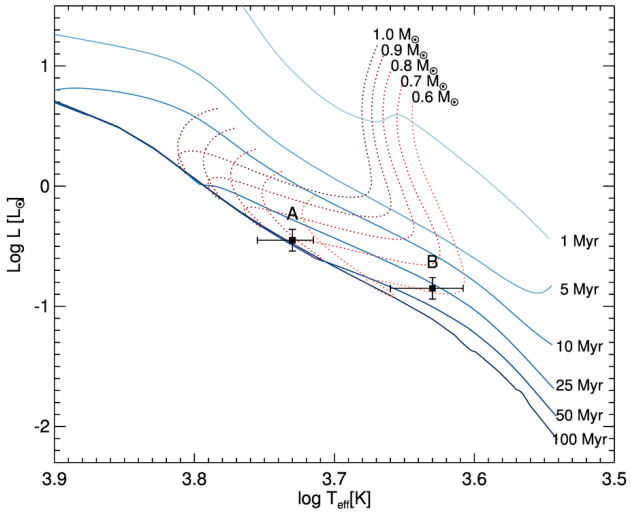

Fig. 4. The position of both components of HD 102077 in an H-R diagram along with the Pisa pre-main-sequence tracks and isochrones (Tognelli et al., 2011) for a metal abundance of Z = 0.005, a helium fraction of Y = 0.273, and a mixing length of ML = 1.68.

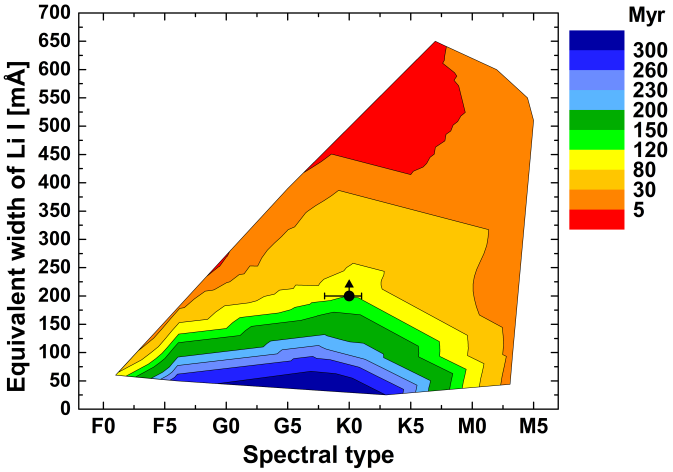

Fig. 5. Li I EW over spectral type. The coloured contours show the age calibration of Zuckerman & Song (2004). The black circle indicates the upper limit of the age of the primary component with spectral type error bars from photometry.

Table 3. Summary of photometric and spectroscopic results.

Property	Value
Spectral type primary	$K0 \pm 1$
Spectral type secondary	$K5 \pm 1$
Photometric period	none significant
Isochrone age (Myr)	> 25
Lithium age (Myr)	< 120
Mean radial velocity (km/s)	17.6 ± 2
$\mu_\alpha * \cos\delta$ (mas/yr)	-137.84 ± 1.26
μ_δ (mas/yr)	-33.53 ± 1.45

3.4.2. Using the lithium I λ6708 Å equivalent width

To determine the stellar age independently from the stellar parameters, the equivalent width (EW) of the Li I λ6708 Å line can be used (Wallerstein & Conti, 1969). The reaction rates of the lithium burning depends on the age of the star and on its mass, and the corresponding effective temperature and young stars exhibit larger Li features than older stars. Although this age estimation method is under discussion because non-steady accretion can heavily affect the Li I depletion (Baraffe & Chabrier, 2010), it is still a commonly used age indicator (e.g. Thomann et al., 2013).
Since the Li I line at 6708 Å is blended with an Fe I line, the line was fitted with a Voigt profile to account for the blending. Using the Voigt fit, the EW was derived. By using the SNR of the spectra as a weight, the average Li EW with error was calculated from the individual EWs derived from each single spectrum. Since the binary does not show WISE IR-excess, disk accretion is unlikely to occur and we do not expect veiling (Lynden-Bell & Pringle, 1974; Kenyon & Hartmann, 1987; Bertout et al., 1988). The resulting Li I EW is 200 ± 4 mÅ which agrees well with the previously measured values for HD 102077 (Song et al., 2002) and its probable third, wider component discovered by König et al. (2003).

In order to determine the stellar age from the derived Li EW, an age calibration is needed. Zuckerman & Song (2004) used eight different stellar associations with calculated Li EWs and independently derived mean age. By doing so, they derived an age calibration of Li I EW over (B-V) and spectral type, allowing a simple placement of object measurements in the calibration.
Figure 5 shows the Li EW measurement of HD 102077 of 200 ± 4 mÅ in the diagram. This corresponds to a maximum age of 120 Myr. The minimum age is not as well constrained as we measure the EW of the combined signal, and the later K-type secondary star is expected to have a smaller EW than the primary. The lithium analysis would benefit from taking the binarity of the system into account. Our spectral resolution and the signal-to-noise ratio are, however, not high enough to disentangle the signal of both stars.

4. Discussion

4.1. Additional companions

In addition to the wide companion candidate described by König et al. (2003), our mass estimate of 2.6 ± 0.8 $M_\odot$ may indicate that HD 102077 has another, so far unknown companion; this is considered because the two K-type stars should be less massive than 1.6 $M_\odot$. This would be in accordance with the classification as RS CVn by Weiler & Stencel (1979), Gurzadian & Cholakian (1992), and Pallavicini et al. (1992). In addition, the 2D cross correlation shows a large radial velocity difference which is in disagreement with the orbital fit, but could be caused by a third component. In contrast, the V-band variability seems to be linked with stellar activity and HD 102077 has also been classified as BY Draconis by several groups (Udalski & Geyer, 1985; Alekseev & Gershberg, 1996). Whether HD 102077 is only active or a spectroscopic binary is thus not clear. Further evidence is needed to answer this question.

4.2. Spectral type derivation

From the i'-z' colours we determined an integrated spectral type of K2V. The spectral type determined with spectroscopic means was $K0/1Vp$ (Anders et al., 1991) and is thus one subclass earlier. This deviation is common in a spectral classification based on two colours. We found the individual spectral types to be $K0 \pm 1$ and $K5 \pm 1$ which are in agreement with $K0/1V$ and $K5V$ derived by Cutispoto (1998). This classification seems to be more reliable than the K4 and K2 determined by Fabricius & Makarov (2000) since the brighter primary star is expected to have the earlier spectral type unless the companion is a white dwarf. We note that the errors of the two spectral types are correlated. An earlier spectral type of the primary star implies a later type for the secondary.

4.3. Revisiting the Hipparcos data for HD 102077

In the original version of the Hipparcos Catalog (ESA 1997) the dataset of HD 102077 = HIP 57269 was solved as a two-component system, with identical proper motions and parallaxes. The separation and position angle are given in Table 1 and have been included in the visual orbital fit; the absolute astrometry given for HIP 57269 in the main Hipparcos Catalog corresponds to component A. The solution quality is grade 'A', indicating the highest possible quality.

The two components of the system have been recognized separately in the Hipparcos raw data via a deviation from the distribution of photon count rate as a function of time from the distribution expected for a single star. For these component systems in the original Hipparcos Catalog, the intermediate astrometric data are hard to interpret, since the reference point for the data is not known a priori because it is a complicated function of the photometric and geometric characteristics of the system, and is different for the two data reduction consortia FAST and NDAC.

In the version of the Hipparcos Catalog by van Leeuwen & Evans (1997), the system was recognized as a double star, but again solved with the standard five astrometric parameter model; the astrometry given in the catalog seems to refer to component A, just as in the original version of the Hipparcos Catalog. Our goal is to re-interpret the Hipparcos Intermediate Astrometric Data, taking the orbital solution derived in the present paper into account, and thereby revising the standard astrometric parameters and in particular the parallax.

We used the Hipparcos Intermediate Astrometric Data (abscissae) from van Leeuwen (2007) and fitted corrections to the standard five astrometric parameters (positions and proper motions in right ascension and declination, respectively, and the trigonometric parallax). Before the fitting, we corrected the abscissae for orbital motion, with the orbital parameters given in Table 3. Since the Hipparcos data are absolute astrometric measurements, the reference point for the orbital motion is the centre of mass of the system, against which both components are seen to be moving. In order to derive the centre of mass of the system, we used mass estimates of $0.9\,M_\odot$ for the primary and $0.7\,M_\odot$ for the secondary.

As expected, the largest adjustment occurs in the proper motions when the orbit is taken into account in the analysis of the Hipparcos data. This is because the Hipparcos measurements are spread out over approximately three years, whereas the orbital period is more than a factor of 10 larger, so that the orbital phase coverage of the Hipparcos measurements is relatively small. Thus, some orbital motion has been presumably subsumed into the proper motions before, whereas the corrected proper motions should be free of orbital motion. The new proper motions are $\mu_\alpha * \cos\delta = -137.84 \pm 1.26$ mas yr^{-1} and $\mu_\delta = -33.53 \pm 1.45$ mas yr^{-1}; we reassess the kinematic membership of HD 102077 to a moving group on the basis of these new proper motions in Section 4.4. The parallax of HD 102077 of 20.59 ± 2.14 mas, however, does not change at all when the orbit is taken into account in the fitting of the Hipparcos abscissae.

We caution that we might have misinterpreted the reference point of the Hipparcos Intermediate Astrometric Data, which would render our newly derived proper motions meaningless. However, we have verified that the parallax result is very robust and does not change at all even if we assume other reference points. So we conclude that the published Hipparcos parallax is correct even in the case of orbital motion.

4.4. Moving group membership

The source HD 102077 was proposed as candidate member of TW Hydrae (Makarov & Fabricius, 2001). However, objections have been raised based on the space motion and weaker-than-expected lithium absorption (Song et al., 2002; König et al., 2003). We now revisit both points.

Our new, high-resolution measurements of the Li EW confirm the lithium absorption value and the comparison of our data to stellar isochrones also suggests a higher age of HD 102077 than is predicted for TW Hydrae.

Anders et al. (1991) measured the radial velocity of HD 102077 in July 1987 and König et al. (2003) in January 2002; we measured the radial velocity in July 2013. The results are 15.9 km/s, 19 ± 3 km/s, and 19.8 ± 0.1 km/s respectively. Another RV-measurement was done by Nordström et al. (2004) who find 16.8 ± 0.3 km/s, but they do not give the epoch. These radial velocity values do not take the orbital motion into account. According to our orbit fit the relative motion of both components was 3.8 km/s in July 1987, 0.6 km/s in January 2002, and 5.0 km/s in July 2013. As in section 3.2.2 we adopt a maximum uncertainty of half the relative motion (e.g. 1.9 km/s for 1987). For the measurement by Nordström et al. (2004) we assume an uncertainty of 2 km/s. The weighted mean of this values gives 17.6 ± 2 km/s.

This RV value together with the newly derived proper motion can be used to calculate the space velocity as well as the kinematic membership likelihood. We derive UVWXYZ Galactic velocities and positions of the binary to be $U = -18.9 \pm 1.1$ km/s, $V = -29.7 \pm 2.5$ km/s, and $W = -11.7 \pm 2.9$ km/s, as well as $X = 17.7 \pm 1.4$ pc, $Y = -44.0 \pm 2.4$ pc, and $Z = 10.1 \pm 2.3$pc and compare these values to those of TWA ($U = -9.9 \pm 4.2$ km/s, $V = -18.1 \pm 1.4$ km/s, $W = -4.5 \pm 2.8$ km/s, and $X = 12.5 \pm 7.1$ pc, $Y = -42.3 \pm 7.3$ pc, $Z = 21.6 \pm 4.2$pc; Malo et al. (2013)). We find that even though the Galactic position of HD 102077 is close to most of the TW Hydrae members its space motion is different. The space motion of HD 102077 also does not fit other young associations (see Fig. 6). To calculate the moving group membership probability quantitatively we use BANYAN II (Bayesian Analysis for Nearby Young AssociatioNs II) (Malo et al., 2013; Gagné et al., 2013) and find a probability of 0.4% of HD 102077 being a member of TWA. Even if the true parallax value happens to be outside of its $3\,\sigma$ confidence region, the kinematic membership probability does not get higher than 10%. Together with the estimated age this strongly suggests that HD 102077 is not a member of TWA. The probability of HD 102077 being a mem-

ber of another young moving group is only non-zero for AB Doradus. With the newly derived system parameters it is about 0.03% and it is thus unlikely even though the age of the binary system matches the age of this moving group better. HD 102077 is most likely a member of the young Galactic field.

5. Summary

Our photometric and spectroscopic measurements made it possible to study various aspects of the young, late type binary HD 102077. We present a new, amended orbit fit with small uncertainties on the orbital elements. Using the revised Hipparcos parallax, we deduce a total system mass of $2.6 \pm 0.8\,M_{\odot}$ which leaves the possibility of HD 102077 having a third, close companion. Further evidence for this hypothesis was found in the 2D cross correlation function of the two high-resolution spectra of HD 102077. They show a large radial velocity difference that is in disagreement with the orbital fit, but which could be caused by a third component. In addition, HD 102077 probably has a wider companion at about 400 AU. We also use the derived orbit to revise the kinematics of the system. We find a proper motion of $\mu_\alpha * \cos\delta = -137.84 \pm 1.26$ mas yr^{-1} and $\mu_\delta = -33.53 \pm 1.45$ mas yr^{-1}, as well as a radial velocity of 17.6 ± 2 km/s.

From the i'-z' colours we determine the spectral type of both components to be $K0 \pm 1$ and $K5 \pm 1$, respectively. We then use this result together with the individual Tycho B_T and V_T colours to estimate an age of the system. We find that HD 102077 is very likely older than 25 Myr, which is in agreement with the lithium equivalent width of 200 ± 4 mÅ and with the absence of circumstellar material. Our results are summarized in Tables 2 and 3.

With the amended kinematic data and the age estimate, we deduce the probability of HD 102077 being a member of one of the young moving groups and find no match. Even the proposed candidate membership of HD 102077 to the TW Hydrae Association is very unlikely.

For future investigation it would be interesting to study the radial velocity orbit of HD 102077 to clearly answer the question whether the system contains a third component.

Acknowledgements. We thank the staff at La Silla observatory for their support as well as Carolina Bergfors for observing 3 epochs of HD 102077 and Felix Hormuth for his help with the analysis of the Lucky Imaging data. In addition, we thank Chad Bender for sharing his 2D cross-correlation code.

References

Alekseev, I. Y., & Gershberg, R. E. 1996, Astrophysics, 39, 33
Anders, G. J., Coates, D. W., Thompson, K., & Innis, J. L. 1991, MNRAS, 252, 408
Baraffe, I., & Chabrier, G. 2010, A&A, 521, A44
Bertout, C., Basri, G., & Bouvier, J. 1988, ApJ, 330, 350
Bessell, M. S. 2000, PASP, 112, 961
Casagrande, L., Schoenrich, R., Asplund, M., et al. 2011, VizieR Online Data Catalog, 353, 9138
Cutispoto, G. 1990, A&AS, 84, 397
Cutispoto, G. 1993, A&AS, 102, 655
Cutispoto, G. 1998, A&AS, 131, 321
Cutri, R. M., & et al. 2012, VizieR Online Data Catalog, 2311, 0
ESA 1997, VizieR Online Data Catalog, 1239, 0
Fabricius, C., & Makarov, V. V. 2000, A&A, 356, 141
Fruchter, A. S., & Hook, R. N. 2002, PASP, 114, 144
Gagné, J., Lafrenière, D., Doyon, R., Malo, L., & Artigau, É. 2013, arXiv:1312.5864
Gregorio-Hetem, J., Lepine, J. R. D., Quast, G. R., Torres, C. A. O., & de La Reza, R. 1992, AJ, 103, 549
Gurzadian, G. A., & Cholakian, V. G. 1992, Ap&SS, 188, 205
Hartkopf, W. I., Mason, B. D., Barry, D. J., et al. 1993, AJ, 106, 352
Hartkopf, W. I., Tokovinin, A., & Mason, B. D. 2012, AJ, 143, 42
Heintz, W. D. 1986, A&AS, 65, 411
Hippler, S., Bergfors, C., Brandner Wolfgang, et al. 2009, The Messenger, 137, 14
Hofmann, R., Blietz, M., Duhoux, P., et al. 1992, European Southern Observatory Conference and Workshop Proceedings, 42, 617
Holden, F. 1965, Publications of Michigan Observatory, 9, 181
Holmberg, J., Nordström, B., & Andersen, J. 2007, A&A, 475, 519
Hormuth, F., Brandner, W., Hippler, S., & Henning, T. 2008, Journal of Physics Conference Series, 131, 012051
Kastner, J. H., Zuckerman, B., Weintraub, D. A., & Forveille, T. 1997, Science, 277, 67
Kaufer, A., & Pasquini, L. 1998, Proc. SPIE, 3355, 844
Kenyon, S. J., & Hartmann, L. 1987, ApJ, 323, 714
Köhler, R., Ratzka, T., Herbst, T. M., & Kasper, M. 2008, A&A, 482, 929
König, B., Neuhäuser, R., Guenther, E. W., & Hambaryan, V. 2003, Astronomische Nachrichten, 324, 516
Kovács, G., Zucker, S., & Mazeh, T. 2002, A&A, 391, 369
Kraus, A. L., & Hillenbrand, L. A. 2007, AJ, 134, 2340
Lynden-Bell, D., & Pringle, J. E. 1974, MNRAS, 168, 603
Makarov, V. V., & Fabricius, C. 2001, A&A, 368, 866
Makarov, V. V. 2003, AJ, 126, 1996
Malo, L., Doyon, R., Lafrenière, D., et al. 2013, ApJ, 762, 88
Mason, B. D., Wycoff, G. L., Hartkopf, W. I., Douglass, G. G., & Worley, C. E. 2011, VizieR Online Data Catalog, 1, 2026
Mazeh, T., Prato, L., Simon, M., et al. 2002, ApJ, 564, 1007
McAlister, H., Hartkopf, W. I., & Franz, O. G. 1990, AJ, 99, 965
Moór, A., Szabó, G. M., Kiss, L. L., et al. 2013, MNRAS, 435, 1376
Müller, A., Roccatagliata, V., Henning, T., et al. 2013, A&A, 556, A3
Nordström, B., Mayor, M., Andersen, J., et al. 2004, A&A, 418, 989
Olsen, E. H. 1994, A&AS, 104, 429
Pallavicini, R., Randich, S., & Giampapa, M. S. 1992, A&A, 253, 185
Plavchan, P., Jura, M., Kirkpatrick, J. D., Cutri, R. M., & Gallagher, S. C. 2008, ApJS, 175, 191
Randich, S., Gratton, R., & Pallavicini, R. 1993, A&A, 273, 194
Rochau, B., Brandner, W., Stolte, A., et al. 2010, ApJ, 716, L90
Rodriguez, D. R., Zuckerman, B., Kastner, J. H., et al. 2013, ApJ, 774, 101
Rossiter, R. A. 1955, Publications of Michigan Observatory, 11, 1
Rousset, G., Beuzit, J.-L., Hubin, N., et al. 1994, Proc. SPIE, 2201, 1088
Schlieder, J. E., Lépine, S., & Simon, M. 2010, AJ, 140, 119
Schlieder, J. E., Lépine, S., & Simon, M. 2012, AJ, 143, 80
Schlieder, J. E., Lépine, S., & Simon, M. 2012, AJ, 144, 109
Shkolnik, E. L., Anglada-Escudé, G., Liu, M. C., et al. 2012, ApJ, 758, 56
Song, I., Bessell, M. S., & Zuckerman, B. 2002, A&A, 385, 862
Thomann, C., James, D. J., Boberg, O. M., Cargile, P., & Aarnio, A. 2013, American Astronomical Society Meeting Abstracts, 221, #250.29
Tognelli, E., Prada Moroni, P. G., & Degl'Innocenti, S. 2011, A&A, 533, A109
Tokovinin, A., Mason, B. D., & Hartkopf, W. I. 2010, AJ, 139, 743
Torres, C. A. O., Quast, G. R., Melo, C. H. F., & Sterzik, M. F. 2008, Handbook of Star Forming Regions, Volume II, 757
Udalski, A., & Geyer, E. H. 1985, Information Bulletin on Variable Stars, 2691, 1
Valenti, J. A., & Piskunov, N. 1996, A&AS, 118, 595
van Dessel, E., & Sinachopoulos, D. 1993, A&AS, 100, 517
van Leeuwen, F., & Evans, D. W. 1997, VizieR Online Data Catalog, 413, 157
van Leeuwen, F. 2007, A&A, 474, 653
Voigt, H.-H. 1988, Abriß der Astronomie.. H.-H. Voigt.4. völlig neu bearbeitete Auflage. BI-Wissenschaftsverlag, Mannheim, F.R. Germany. 18+534 pp. Price DM 54.00 (1988). ISBN 3-411-03148-4.,
Wallerstein, G., & Conti, P. S. 1969, ARA&A, 7, 99
Weinberger, A. J., Anglada-Escudé, G., & Boss, A. P. 2013, ApJ, 762, 118
Weiler, E. J., & Stencel, R. E. 1979, AJ, 84, 1372
Weise, P., Launhardt, R., Setiawan, J., & Henning, T. 2010, A&A, 517, A88
Worley, C. E. 1978, Publications of the U.S. Naval Observatory Second Series, 24, 1
Zechmeister, M., Kürster, M. 2009, A&A, 496, 577
Zuckerman, B., & Song, I. 2004, ARA&A, 42, 685
Zuckerman, B., Rhee, J. H., Song, I., & Bessell, M. S. 2011, ApJ, 732, 61

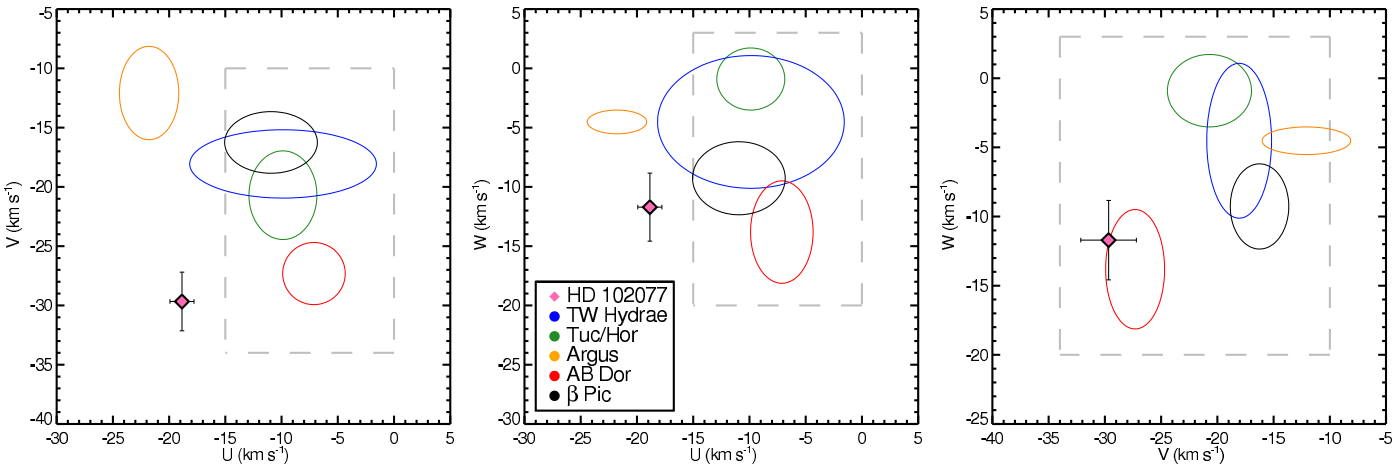

Fig. 6. 2D projections of the UVW space velocities compared to well known moving groups, including TWA. The dashed grey box is taken from Zuckerman & Song (2004) and shows the region of UVW space typically occupied by nearby young stars. The UVW velocities of the young moving groups are taken from Malo et al. (2013), the 2σ uncertainties are plotted. HD 102077 is clearly not a member of any of these groups.